Distribution Agreement

In presenting this thesis as a partial fulfillment of the requirements for a degree from Emory University, I hereby grant to Emory University and its agents the non-exclusive license to archive, make accessible, and display my thesis in whole or in part in all forms of media, now or hereafter now, including display on the World Wide Web. I understand that I may select some access restrictions as part of the online submission of this thesis. I retain all ownership rights to the copyright of the thesis. I also retain the right to use in future works (such as articles or books) all or part of this thesis.

Nicole Lulkin April 12, 2022

Investigating Novel SARS-CoV-2 Inhibitors: Identification of Potent SARS-CoV-2 Antiviral Compounds and Development of a Luciferase-Based Reporter Vector for Papain-Like Protease Inhibition

by

Nicole Lulkin

Dr. Stefan Sarafianos
Adviser

Department of Biology

Dr. Stefan Sarafianos
Adviser

Dr. Philip Tedbury
Committee Member

Dr. Dieter Jaeger
Committee Member

2022

Investigating Novel SARS-CoV-2 Inhibitors: Identification of Potent SARS-CoV-2 Antiviral Compounds and Development of a Luciferase-Based Reporter Vector for Papain-Like Protease Inhibition

By

Nicole Lulkin

Dr. Stefan Sarafianos
Adviser

An abstract of
a thesis submitted to the Faculty of Emory College of Arts and Sciences
of Emory University in partial fulfillment
of the requirements of the degree of
Bachelor of Science with Honors

Biology Department

2022

Abstract

Investigating Novel SARS-CoV-2 Inhibitors: Identification of Potent SARS-CoV-2 Antiviral Compounds and Development of a Luciferase-Based Reporter Vector for Papain-Like Protease Inhibition

By: Nicole Lulkin

The rapid spread of SARS-CoV-2 across the world has taken a tremendous toll on all sectors of society and led to high mortality rates. While vaccines remain the most effective way to decrease hospitalizations and deaths due to SARS-CoV-2, they are challenging to distribute globally, demonstrate decreased efficacy against emerging SARS-CoV-2 variants, and have lower benefits in populations such as younger children and immunocompromised individuals. Therefore, antiviral drugs are needed alongside vaccines as a treatment for SARS-CoV-2.

I screened twenty-one novel antiviral compounds for inhibition of SARS-CoV-2 viral replication. Four of these novel compounds were nucleoside analogues targeting SARS-CoV-2 RNA-dependent RNA polymerase (non-structural protein 12) and seventeen targeting the SARS-CoV-2 papain-like protease (PLpro). To safely screen the potential antivirals in BSL2 biocontainment facilities, I primarily used a SARS-CoV-2 replicon system in transient and stable cell-line formats. These screening systems allowed me to study the effects of the SARS-CoV-2 exonuclease nsp14 and remdesivir (RDV) resistance-associated nsp12 mutations on nucleoside analogue potency. I also developed a PLPro reporter vector to facilitate future PLpro antiviral compound validation and in-depth mechanistic examinations.

Collectively, our study revealed two small molecule PLpro-inhibitors with sub-micromolar EC_{50} values and a PLpro Proteolysis Targeting Chimera (PROTAC) with a <1.5 μM EC_{50} value. We also determined that despite their predicted benefits, the PROTAC moieties we screen by more than 14-fold. Lastly, we found that the sensitivity of the PLpro cell-based luciferase assay at this stage did not allow for dose-response analysis of antiviral compounds. With antiviral drugs continuing to be developed against SARS-CoV-2, the inhibitory compounds identified in this study and analysis of various compound screening methods can inform the ongoing search for COVID-19 therapeutics.

Investigating Novel SARS-CoV-2 Inhibitors: Identification of Potent SARS-CoV-2 Antiviral Compounds and Development of a Luciferase-Based Reporter Vector for Papain-Like Protease Inhibition

By

Nicole Lulkin

Dr. Stefan Sarafianos
Adviser

A thesis submitted to the Faculty of Emory College of Arts and Sciences
of Emory University in partial fulfillment
of the requirements of the degree of
Bachelor of Science with Honors

Biology Department

2022

Acknowledgments

First, I would like to thank Dr. Stefan Sarafianos for giving me the opportunity to grow as a scientist in his laboratory. I further want to thank him for entrusting me with a variety of projects and experiments and believing in my research abilities. His involvement and support, both academic and personal, has shaped my experience at Emory.

Next, I would like to thank Dr. Shuiyun Lan, for his direct mentorship and guidance. I greatly appreciate his patience and skills as a researcher and teacher. His hard work ethic and passion for research motivated me to set high standards for my own research and work towards reaching them. The knowledge I have gained by shadowing and working with Lan will continue to illuminate my future work.

I would also like to thank Dr. Philip Tedbury for his helpful feedback and advice on both my scientific writing and experimentation. Through my conversations with him, I have increased my critical thinking and data analyzation skill set.

Fourth, I would like to thank Dr. Dieter Jaeger for encouraging my interest in Biology through his Human Physiology course. I also appreciate his involvement on my committee along with Dr. Sarafianos and Dr. Tedbury.

Furthermore, I would like to thank additional members of the Sarafianos Lab who have all supported me throughout different parts of my research journey and will list them here in no particular order: Maria Cilento, Ciro Carrillo, Emerson Boggs, Dr. William Cantara, Dr. Yee Ong, Dr. Ryan Slack, Huanchun Zhang, Alexa Snyder, and Will McFadden.

In addition, I appreciate the Wei-Shau Hu Lab, Schinazi Lab, Kovari Lab and Progenra for their reagent contributions.

Finally, I would like to thank my mother, father, and sister along with my friends for being my cheerleaders and providing me with moral support. I could not have completed my research without their unrelenting encouragement.

Table of Contents

1. Introduction

1.1: SARS-CoV-2 Epidemiology and Prevalence

Severe acute respiratory coronavirus 2 (SARS-CoV-2) is the virus responsible for coronavirus disease 2019 (COVID-19). SARS-CoV-2 was first detected in Wuhan, in the Hubei Providence of China, in December 2019 and has since spread across the world [1]. COVID-19 was initially deemed an epidemic and then a pandemic in March 2020, due to the widespread cases of COVID-19 [2]. The COVID-19 pandemic is the first known pandemic to be started by a coronavirus. Since March 2020, the efforts to contain COVID-19 have led to schools shutting down, country lockdowns and sacrifices across all sectors of society. Although COVID-19 restrictions are beginning to be lifted, the mental health and economic crises resulting from this pandemic continue to impact populations.

Despite public health and government endeavors to prevent the spread of COVID-19, this disease has continued to proliferate due to its highly infectious nature. As of March 18th 2022, there have been 464,809,377 confirmed COVID-19 cases globally and 6,159,474 deaths [3]. In the United States alone as of, 79,465,958 cases of COVID-19 have been reported along with 960,935 deaths since this date [3]. Densely populated areas have especially high rates of COVID-19 infections. Besides the serious health impacts of COVID-19, this pandemic has also disproportionately impacted the elderly, people with disabilities, youth and indigenous people while exacerbating pre-existing racial and socioeconomic inequalities. Therefore, it is essential that the scientific community works together to advance treatment options against COVID-19.

1.2: SARS-CoV-2 Phylogeny and Disease Characteristics

Coronaviruses (CoVs) belong to a large group of envelope, non-segmented positive-sense RNA viruses and can cause different diseases in both mammals and birds [4]. The *Coronaviridae* family are a part of the *Nidovirales* order and contains the alpha, beta, gamma and delta coronavirus genera [4]. Coronaviruses, including SARS-CoV-2, have larger RNA genomes in comparison to other RNA viruses, ranging from 26,000 to 32,000 bases [5]. SARS-CoV-2 in particular has a 30,000 base genome with a 5' terminal cap and 3' polyA tail tail [6]. In contrast, RNA viruses such as the picornavirus has a genome between 7,100 and 8,900 bases in length while the flaviviruses have genome lengths of 11,000 bases [7]

COVID-19 is part of the *Betacoronavirus* genus along with the zoonotic coronaviruses severe acute respiratory virus (SARS-CoV) and middle east respiratory syndrome coronavirus (MERS-CoV) [8]. SARS-CoV emerged in late 2002 while MERS-CoV spread in 2012, however, neither of these viruses resulted in a pandemic [9]. SARS-CoV-2 has a replication number, number of secondary transmission events from one infected person, R_0 of 2·5, while SARS-CoV has an R_0 of 2·0-3·0 and MERS-CoV has an R_0 of 0·9 [9].

SARS-CoV-2 is more infectious than the other zoonotic coronaviruses because it replicates in the upper respiratory tract leading to greater transmissibility [10]. This virus also replicates in the lower respiratory tract and other organ systems such as the GI tract [10]. Many factors, including age and disease history, impact the severity of COVID-19 symptoms. While some individuals are asymptomatic, others suffer from flu-like symptoms, including fever, non-productive cough, and lethargy [6]. In older and immunocompromised patients, symptoms can even progress to multi-organ failure and septic shock [11].

1.3 SARS-CoV-2 Genome

SARS-CoV-2 has 13-15 open reading frames (ORFs) and 38% GC content [12]. Upon the entry of SARS-CoV-2 into cells, genomic RNA (gRNA) is used to code for 16 non-structural proteins (nsps) that make up the initial two-thirds of the SARS-CoV-2 genome downstream from the 5'-end [13]. Open Reading Frames (ORFs) 1a and 1b contain these nsp sequences. ORF1a is translated into polypeptide 1a before being cleaved into 11 nsps, while ORF1b is translated into polypeptide 1ab and subsequently cleaved into 15 nsps by viral proteases [13]. In the final one-third of the SARS-CoV-2 genome, four essential structural proteins, including spike (S), nucleocapsid (N), envelope (E), and membrane (M) proteins, along with accessory protein-coding open reading frames, are encoded [13].

The SARS-CoV-2 non-structural proteins have 85% amino acid sequence similarity to SARS-CoV [14]. Except for the S protein these two viruses share 90% of the same amino acid sequence [14]. The S protein of SARS-CoV-2 has less than 75% nucleotide sequence similarity compared to other SARS-CoV viruses and therefore differs in host entry mechanisms [15]. A 4 amino acid insertion between the two subunits S1 and S2 of the S protein accounts in part for such differences [14].

The non-structural proteins have been studied to have a variety of essential roles in the life cycle of SARS-CoV-2. Non-structural proteins (nsps) often interact to carry out vital enzymatic functions [5]. In this research study, three different non-structural proteins will be studied in greater detail, including nsp3, nsp14 and nsp12, to determine the effects of antiviral compounds on them.

As SARS-CoV-2 continues to spread across the world, this deadly virus has acquired certain novel mutations that have led to higher infectivity and immune system evasion capabilities. The mutation rate of SARS-CoV-2 has been calculated to be about 10^{-3} substitutions per year per site

[16]. SARS-CoV-2 viruses that acquire specific conserved mutations increase in prevalence in certain populations and are known as variants. The Alpha (B.1.1.7), Beta (B.1.351), Gamma (P.1) and Delta (B.1.617.2) variants are currently referred to as Variants of Concern by the World Health Organization (WHO) because of 1 or more mutations that can affect their infectivity or disease presentation or response to treatments/vaccine efficacy [17]. The rise in these variants shows a need for more research efforts devoted to identifying how highly conserved mutations can impact the interactions between non-structural and structural proteins and affect viral properties.

1.4: SARS-CoV-2 Mechanism of Infection and Replication Process

The replication process of SARS-CoV-2 begins with the binding of the S protein to the angiotensin-converting enzyme 2 (ACE2) receptor [18]. The S protein binding to ACE2 and cleavage by proteases, such as TMPRSS2 on the cell surface or cathepsin L in the endosome, that allows the S2 domain of S protein to be revealed [15, 19]. The exposed S2 domain then inserts into the host membrane and drives fusion of the virus and host membranes, allowing the viral genomic RNA (gRNA) to enter the cytoplasm of the cell. ORF1a and ORF1b are translated into pp1a and pp1ab polyproteins (the latter a consequence of ribosome slippage during translation) and then processed by the viral proteases to release the 16 nsps. Pp1a, 4405 amino acids, is cleaved into nsp1-11, while pp1ab, 7096 amino acids, is cleaved into nsp12-16 [20].

The nsps have enzymes necessary for the formation of the replication and transcription complex (RTC) with RNA-dependent RNA polymerase [19] [20]. The RTC replicates viral RNA by transcribing positive-strand gRNA into negative-strand gRNA which creates new gRNA and negative-strand subgenomic RNA templates [21]. These templates are subsequently translated into structural proteins and accessory proteins [21]. In endoplasmic-reticulum bound ribosomes,

structural proteins including the spike, membrane, and envelope proteins are translated. The nucleocapsid protein is translated in cytoplasmic ribosomes. The nucleocapsid protein then combines with positive-strand genomic RNA to create a nucleoprotein complex. Finally, the nucleoprotein complex merges with the translated structural proteins into a complete viral particle in the ER-Golgi apparatus compartment and is excreted extracellularly via the secretory pathway [22]. Non-structural proteins are therefore essential for the reproduction of the virus and serve as therapeutic targets for antiviral compounds.

1.5: SARS-CoV-2 Viral Proteases

Two viral proteases cleave the SARS-CoV-2 non-structural proteins. The main protease of SARS-CoV-2 is nsp5 and called Mpro or 3C-like protease (3CLpro) due to its chymotrypsin-like folds. It is a 30 kDa and a three-domain cysteine protease that is highly conserved among the coronaviruses [19]. 3CLpro has a catalytic dyad consisting of Cys145 and His41 and cuts at 11 different sites; 3CLpro cleaves nsp4-nsp11 of pp1a and nsp4-nsp16 of pp1ab [23]. It has a conserved cleavage site of X-L/F/M-Q↓G/A/S-X [23]. Without cleavage by 3CLpro, coronaviruses cannot replicate making this protease an important target of antiviral compounds.

The second viral protease is a part of nsp3. Nsp3 is the largest SARS-CoV-2 non-structural protein and contains the papain-like protease (PLpro) region that cleaves the translated polyprotein at 3 different junctions, separating nsp1, nsp2, and nsp3. PLpro consists of 315 residues has a catalytic triad consisting of Cys111, His 272, and Asp286 [23]. This protease recognizes a conserved cleavage site, LXGG↓XX; PLpro cleaves at LNGG↓AYTR between nsp1 and nsp2, LKGG↓APTK between nsp2 and nsp3, and LKGG↓KIVN between nsp3 and nsp4 [23].

While PLpro shows significant homology in SARS-CoV and SARS-CoV-2, only the SARS-CoV-2 PLpro has been studied to suppress innate immune functions in host cells. Such functions are due to its high binding affinity for Interferon Stimulated Gene 15, an important protein in the innate immune response to SARS-CoV-2 [24]. By binding to ISG15, PLpro prevents ISGylation and therefore the modulation of necessary proteins in the interferon-mediated immune pathway cascade [24]. Furthermore, PLpro inhibits cellular ubiquitination which is necessary for proteasomal degradation [24]. SARS-CoV-2 PLPro has a higher affinity for ISGylated proteins in comparison to ubiquinated substrates unlike SARS-CoV PLpro due to additional residues that allow for greater binding specificity [25].

PLpro is therefore an essential component of the SARS-CoV-2 replication cycle and immune system evasion. This protease is also a favorable target for antiviral compounds because of its interactions with nsp2, ORF3a proteins, ORF9b proteins, nsp4, nsp12, ORF7a proteins and nsp6 [26].

1.6: SARS-CoV-2 N-terminal 3'-to-5' Exoribonuclease (ExoN)

Nsp14 is a bifunctional non-structural protein that contains an N-terminal 3'-to-5' exoribonuclease (ExoN) that removes nucleotides from the 3' end along with a C-terminal N7-methyltransferase (N7-MTase) domain [27]. The exoribonuclease works on both single-stranded and double-stranded RNA by metal-ion dependent activity [28]. This enzyme is a member of the DEDD superfamily which includes proteins characterized by a core of four invariant acidic amino acids (Asp/Glu residues) that compose three different conserved sequences (motifs) [29]. The ExoN works with nsp10 and nsp12 to repair any incorrectly-incorporated nucleotides which are then excised out [30]. The N7-MTase allows for CoV mRNA to have a 5'-terminal cap structure because guanine-N7-methylation is necessary for cap recognition [30]. N7-MTase

activity is also dependent on the N-terminal ExoN domain being intact despite separate enzymatic domains and functions [30].

Coronaviruses have larger genomes than other RNA viruses due to their ExoN-mediated proofreading mechanisms [30]. RNA viruses without such proofreading capabilities have limited RNA sizes due to increased rates of mutation because of the limited RNA-dependent RNA polymerase fidelity [30]. ExoN allows SARS-CoV-2 to have lower mutation rates than other RNA viruses, allowing SARS-CoV-2 to maintain fitness despite its large genome size [31]. Nsp14 is therefore crucial for nucleoside monophosphate excision from nucleic acids which is necessary for proofreading, other RNA viruses do not have such a domain [27]. In a study with HCoV-229E mutants with non-functional Exonuclease activity, replication was impaired. Viral RNA was reduced by 180-fold in the HCoV-229E mutants in comparison to wild-type HCoV-229E [28]. Furthermore, increased nucleotide misincorporation was observed in the absence of ExoN activity, demonstrating the necessity of this function to the maintenance of replication fidelity and viral viability [28].

The ExoN activity of the coronaviruses may also hinder the efficacy of nucleoside analogue antiviral compounds due to its excision function. In a 2018 study, it was discovered that Murine Hepatitis Virus (MHV) mutants without ExoN proofreading activity had a 4.5-fold EC_{50} decrease from WT MHV following incubation with antiviral compound RDV [32]. Such increased sensitivity to RDV without functional ExoN abilities shows that nucleoside analogues such as RDV can be removed by ExoN leading to lower drug potency.

Furthermore a recent study including SARS-CoV-2 and MERS-CoV mutants without ExoN proofreading capabilities revealed that ExoN activity is required for replication, suggesting that the ExoN activity may be a viable antiviral target [30]. ExoN activity needs to be studied in

greater detail in SARS-CoV-2 to determine its impact on resistance to antiviral nucleoside analogue compounds and viral replication.

1.6 SARS-CoV-2 RNA-dependent RNA Polymerase

Non-structural protein 12 encodes viral RNA-dependent RNA polymerase (RdRp) which is a key member of the coronavirus replication and transcription complex (RTC). Within the Coronaviruses, the core of the RTC is formed by nsp12 complexed with nsp7 and nsp8 cofactors to perform the necessary transcription functions [33].

RdRp has high potential as a target of SARS-CoV-2 inhibitors because it is distinct from host cell machinery, reducing any side-effects from targeting compounds. Furthermore, this protein has active catalytic motifs that have high sequence conservation among RNA viruses allowing for potential repurposing of drugs [34] . RdRp is essential for viral genome replication, making it an especially attractive target of antiviral therapies.

1.7: SARS-CoV-2 Small Molecule Inhibitors

Multiple COVID-19 mRNA vaccines have been authorized by the U.S. Food and Drug Administration (FDA), resulting in lower hospitalization and death rates. However, as SARS-CoV-2 continues to mutate, various emerging variants harbor mutations that decrease COVID-19 vaccine efficacy and protection against the virus. In B.1.1.7 viral isolates, the neutralizing effects of the vaccine decreased by two-fold [35]. Furthermore, various mutations in the B.1.51 variant of SARS-CoV-2 such as E484K and N501Y in the spike-protein led to 1- to 3- fold decreases in vaccine efficacy [35]. While vaccines remain the best defense against COVID-19, they are also difficult to distribute around the world increasing the time to achieve herd-immunity [19].

Therefore, it is vital that researchers examine therapeutic alternatives such as small molecule inhibitors that can inhibit SARS-CoV-2 replication.

Small molecule inhibitors include a variety of antiviral compounds that can be repurposed for use against SARS-CoV-2. Already, remdesivir (RDV), which was developed for treatment of the Ebola virus has been shown to inhibit SARS-CoV-2 RdRp (IC50 = 0.77 μM) and was authorized by the FDA for SARS-CoV-2 treatment [36]. Multiple randomized controlled trials with COVID-19 patients showed that treatment with RDV leads to a 31% faster recovery time [36]. RDV, is a nucleoside analogue (NA) that acts as a high affinity substrate for viral RdRp. Like other prodrugs, this compound is metabolized enzymatically to its active 5'-triphosphate form (GS-441524) once it enters host cell [37].

The structural conservation of RdRp makes this protein a very effective target of antiviral therapies, despite potential resistance due to the nsp14 N-terminal domain ExoN of Coronaviruses. This exonuclease has the potential to decrease RDV effectiveness due to its proofreading capabilities. In a research study with both wild-type and exonuclease-knockout (ExoN (-)) murine hepatitis virus, ExoN (-) virus had a 100-fold reduction in viral replication [32]. Therefore, it is essential to screen various other RdRp-targeting small molecule inhibitors alongside RDV to see if there are similar exonuclease-mediated decreases in inhibition in SARS-CoV-2.

Furthermore, multiple mutations in nsp12 have been studied to result in partial-RDV resistance. In a 2018 study, it was discovered that two nsp12 mutations in MHV, F476L and V553L, resulted in 2.4 and 5.0-fold resistance respectively along with a combined 5.6-fold resistance against RDV [32]. The substitution of a bulky leucine group for phenylalanine at residue 476 was predicted to result in more rigid base-pairing to template nucleotides, reducing

the ability of GS-5734 to be incorporated into the growing RNA chain [32]. Meanwhile, the mutation at amino acid 480 has been predicted to impact active-site catalytic activities [32]. Studying whether such resistance against RDV along with novel nucleoside analogues is seen in SARS-CoV-2 is an important step towards developing therapeutic measures against COVID-19.

Viral protease, PLpro, is another target of small molecule inhibitors in previous efforts against RNA viruses. In a 2018 study, disulfiram was shown to competitively inhibit PLPro in SARS-CoV and MERS-CoV through zinc-bound cysteine targeting action [38]. Multiple non-covalent and covalent small molecule inhibitors have high effectiveness against SARS-CoV PLpro, showing that antiviral compounds against PLpro can serve as potent inhibitors [39]. It is essential that novel PLpro inhibitors continue to be screened for SARS-CoV-2 therapeutic purposes.

1.8: SARS-CoV-2 Proteolysis Targeting Chimeras (PROTACS)

Proteolysis targeting chimeras (PROTACS) are emerging as another powerful treatment against SARS-CoV-2, with many advantages in comparison to traditional small molecule inhibitors. PROTACS were first developed in 2001 by the Crews and Deshaies labs and have since been modified to increase host-cell permeability and potency [40]. Since their emergence, PROTACS have been used to treat both cancer diseases and viral diseases [[40]. These compounds consist of two binding regions, for an E3 ubiquitin ligase and protein of interest (POI), along with a linker that joins these two subunits together. PROTACS make use of the ubiquitin proteasome system, and suppress protein function by degradation rather than by inhibiting its activity [13]. Once PROTACS enter the host cell, a trimer forms consisting of the POI, E3 ubiquitin ligase, and E2 with ubiquitin. The ubiquitin molecule is then attached to the

POI, leading the E2 ligase to dissociate. Another E2 ligase will bind to the E3 ligase and repeated action forms chains of ubiquitin on the POI that direct it to the proteosome to be degraded.

PROTACS are a highly effective therapeutic alternative to small molecule inhibitors due to this catalytic mode of action which allows them to be used in lower concentrations [40]. PROTACS represent a promising drug development field in which inhibitors can be created through modifications of a protein-of-interest binders that did not previously demonstrate inhibitory protein activity. These inhibitors dissociate following the poly-ubiquitination of the POI, if binding non-covalently, and can be recycled by the host-cell. Furthermore, they can be used against drug-resistant targets that cannot be treated by inhibitors with enzymatic modes of action [13]. PROTACS also have higher selectivity in comparison to traditional inhibitors making them a very promising measure against SARS-CoV-2 [13]. There is a need to continue to test novel SARS-CoV-2 targeting PROTACS as this field continues to grow.

1.9: SARS-CoV-2 Replicon System

To study the effects of antiviral compounds on SARS-CoV-2 variants, the replicon system has been developed. Live viral studies with antiviral therapeutics require the use of biosafety level-3 (BSL3) facilities which limits laboratories from performing urgent COVID-19 treatment screening protocols. Live viruses are highly infectious and transmissible, while the replicon is noninfectious and still maintains genomic replication functions.

By creating a non-infectious SARS-CoV-2 replicon without the S, E, and M gene, this virus can be studied with lower biosafety concerns. Also, replicons can be made with specific mutations found in SARS-CoV-2 variants and knockout genes that allow the impacts of such mutations and genes on replication rates to be researched. Replicons can transcribe mRNA

comparable to the wild-type virus and are constructed in bacterial artificial chromosomes (BAC) [41].

The replicon used in this study includes a nano-luciferase gene that allows us to quantify viral replication efficiency and inhibition due to antiviral compounds [41, 42]. It also contains unique restriction enzyme sites that allow for replicon modifications such as the addition and deletion of genes and mutations [41].

Figure 1.1 Replicon construction overview. WT SARS-CoV-2 ORF1a, ORF1b, and N were inserted in a BAC along with the necessary promoters and transcriptional regulatory sequences to allow for genomic replication. Enhanced green fluorescent protein (eGFP), neomycin phosphotransferase (Neo^R), and Nluc replaced M, E, S, and most accessory ORF proteins to identify gene expression. Adapted from "Subgenomic SARS-CoV-2 replicon and reporter replicon cell lines enable ultrahigh throughput antiviral screening and mechanistic studies with antivirals, viral mutations or host factors that affect COVID-19 replication," by S. Lan, et al., 2021, bioRxiv [41]

1.10: SARS-CoV-2 Cell-Based Luciferase Complementation Assay

The cell-based luciferase assay developed by researchers in the Wei-Shau Hu Lab can also be used to study SARS-CoV-2 inhibition. Compound screening methods such as live viral studies and replicon-based systems do not allow for the targeting of a specific protein. By making use of such a reporter assay, the effects of inhibitors on a single viral enzyme can be studied rather than on multiple viral non-structural proteins, which specifies their mechanism of action.

Furthermore, this reporter assay allows for cytotoxicity effects to be differentiated from drug-caused inhibition. In a replicon-based system, inhibition by antiviral compounds and cell cytotoxicity leads to low luciferase signaling, making it difficult to distinguish between these effects. With the cell-based luciferase assay, such a problem is not encountered since cell cytotoxicity leads to lower luciferase signaling while high luciferase signaling can be attributed to inhibition of the viral protease.

This assay uses the pLVX-Puro-HIV-1 lentiviral vector that allows for constitutively expression of a gene and can be transfected in 293T eukaryotic cells [43]. To examine the various inhibitory effects of protease-inhibitor compounds, a protease gene sequence and its specific cleavage site, framed by two luciferase sequences, are included in the vector. Upon cleavage by the viral protease, luciferase signaling decreases.

In Wei-Shau Hu's SARS-CoV-2 reporter assay, the efficacy of various 3CLpro inhibitors was examined [44]. This novel luciferase complementation reporter assay confirmed different antiviral compound activities previously studied in virus-infected cell lines, showing that it is an effective tool for screening antiviral compounds [44].

2. Material and Methods

2.1: Plasmids and Replicons

WT, ExoN(-) and RDV-resistant SARS-CoV-2 replicons were created in the Sarafianos Lab by Shuiyun Lan. The replicons do not have structural proteins S, M, and E. These coding sequences are replaced with reporter sequences and selectable markers [41]. All other genomic RNA and proteins necessary for replication are conserved in the replicon including ORF1a, ORF1b and body transcription regulatory sequences (TRS-B) that precede ORFs [41]. The 5'

untranslated region (UTR) also contains leader transcription regulatory sequences (TRS-L) which are necessary for the replication of SARS-CoV-2 RNA [41].

The replicon RNA is cloned into pBelobAC11 (NEB) [41]. ExoN(-) replicons have two active site mutations in nsp14, D90A and E92A, that make this enzyme nonfunctional. RDV-resistant replicons have two active site mutations in nsp12, F480L and V557L, have been shown to confer RDV resistance in MHV [32].

3CLpro reporter vectors were generously donated from the Wei-Shau Hu Lab. The donated lentiviral vectors were pLVX-Puro-HIV vectors with an inserted WT SARS-CoV-2-Mpro sequence, NanoBiT luciferase sequences encoding SmBiT and LgBiT, and green fluorescent protein (GFP).

2.2: Cell Lines

HEK 293T/17 cells (human embryonic kidney 293 cells) were sourced from the American Type Culture Collection (ATCC). 293T/17 cells were chosen as the human cell line for transfection with SARS-CoV-2 replicon due to their high transfection and protein expression efficiency [45]. Cells were cultured in Dulbecco's Modified Eagle Medium (DMEM) supplemented with 1 mM sodium pyruvate (Gibco), 10% fetal bovine serum (FBS, Gibco), non-essential amino acids solution (NEAA mixture 100X, Gibco), 2mM L-glutamine (Gibco), 100 U/mL penicillin, and 100 μg/mL streptomycin. Cells were maintained at 37°C in a 5% CO_2 – humidified incubator.

SARS-2-replicon expressing human embryonic kidney cells (293T-SARS-2R_GFP_Neo^R_NL) were cultured in Dulbecco's Modified Eagle's Medium (DMEM) supplemented with 1 mM sodium pyruvate (Gibco), 1% fetal bovine serum (FBS, Gibco), non-

essential amino acids solution (NEAA mixture 100X, Gibco), 2mM L-glutamine (Gibco), 100 U/mL penicillin, and 100 μg/mL streptomycin. Cells were maintained at 37°C in a 5% CO_2 – humidified incubator.

The 293T-SARS-2R_GFP_Neo^R_NL cell line was generated by transfection of human embryonic kidney cells (HEK 293T) with a Wuhan-Hu-1-based SARS-CoV-2 replicon.

2.3: Compounds

Four novel nucleoside analogue antiviral compounds from the Schinazi Lab, Emory School of Medicine, at 40 mM in DMSO were obtained (RDRP-1, RdRp-2, RdRp-3 and RDRP-4). These compounds target RdRp through RNA synthesis termination upon their incorporation in the growing RNA chain. The Schinazi Lab has been instrumental in their production of antiviral agents and hold 22 New Drug Application (NDA) approvals.

Ten novel PLpro-targeting antiviral compounds were obtained from the Kovari Lab (40 mM in DMSO). These drugs (PL-0 – PL-9) are designed to inhibit PLpro enzymatically.

Eight novel PLpro-targeting antiviral compounds (PR-1, PR-2, PR-3, PR-4, PR-5, PR-6, PR-7 and PR-8) were also obtained from the Progenra company (10 mM in DMSO). PR-1 is a covalent small molecule inhibitor that was modified through the attachment of linkers to make PR-2 which is a small molecule PROTAC ligand. PR-2 was then the basis for covalent PROTAC PR-3 with a CRBN E3 ligase. PR-4 is a non-covalent small molecule that was modified to create non-covalent PROTACS PR-5 (with CRBN ligase) and PR-6 (with Progenra's E3 ligase). PR-7 (modified PR-2) and PR-8 are both covalent PROTACS with Progenra's E3 ligase. The Progenra small molecules are able to enzymatically inhibit PLpro, while their PROTAC counterparts are intendeddegrade PLpro through the cell's proteosome-ubiquitin degradation mechanisms.

Remdesivir (#30354 from Cayman Chemicals) is a known RdRp inhibitor (EC_{50} = 0.77 μM) that was used as a positive control across multiple experiments to determine inhibition efficacy of the novel compounds.

2.4: RdRp Dose-Response Antiviral Activity Assay (EC_{50})

293T-17 cells were seeded into 6-well plates (1.2 x 10^6 cells/well) (Figure 2.1). Following 24 hours, WT and ExoN(-) mutant replicons were transfected into the 293T-17 cells using 1 μg replicon plasmid/well, 2.4μL/well jetPRIME transfection reagent (Polypus) and 200 μL/well of jetPRIME transfection buffer Polypus), and 0.2 μg/well of Nucleocapsid plasmid (N), following the manufacturer's instructions (Figure 2.1). 24 hours following transfection, cells were washed with DPBS (Sigma-Aldrich) and removed from 6-well plates by trypsinization. Transfected cells were then pelleted and resuspended in DMEM at a concentration of (8 x 10^5 cells/mL).

Stock solutions of RDRP-1, RdRp-2, RdRp-3, and RDRP-4 were made at a concentration of 80 μM in DMEM, then mixed 1:1 in 96-well plates with trypsinized transfected cells for a high concentration of 40 μM on final plating. RDV was used as a positive control to inhibit replicon activity and was diluted to a final high concentration of 0.3 μM on final plating. Seven three-fold dilutions starting from 40 μM (0.3 μM for RDV) with three replicates per dilution were performed for all compounds (Figure 2.1). Media with 0.2% DMSO was used as a negative control. Luciferase activity was measured 48 hours after compound addition using the Nano-Glo Luciferase Assay System (Promega) (Figure 2.1). Percentage inhibition was calculated for each compound sample using transfected cells with DMSO as 0% inhibition. Percentage inhibition values were then plotted against compound concentrations on a log-scale in GraphPad Prism 9

and analyzed for EC_{50} values using log(agonist) vs. response – Find ECanything- nonlinear slope equation with F = 50.00 and top constraint = 100.0 while bottom constraint = 0.000.

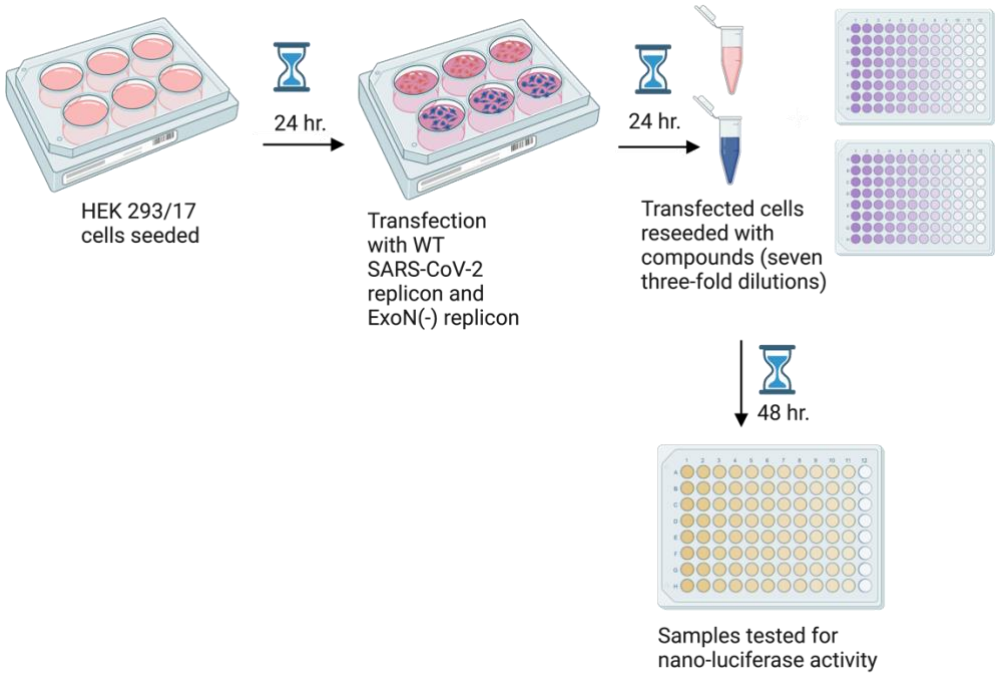

Figure 2.1 Luciferase assay for HEK 293T-17 cells with RdRp antiviral compounds 293T-17 cells were transfected with WT SARS-CoV-2 and ExoN(-) replicons before incubation with novel RdRp antiviral compounds (RDRP-1, RdRp-2, RdRp-3 and RDRP-4). Red cells indicate transfection with WT-SARS-CoV-2 replicon. Blue cells indicate transfection with ExoN(-) SARS-CoV-2 replicon.

Compounds RDRP-4 and RdRp-2 were further screened with WT, ExoN(-) and RDV-resistant replicons using the methods described above.

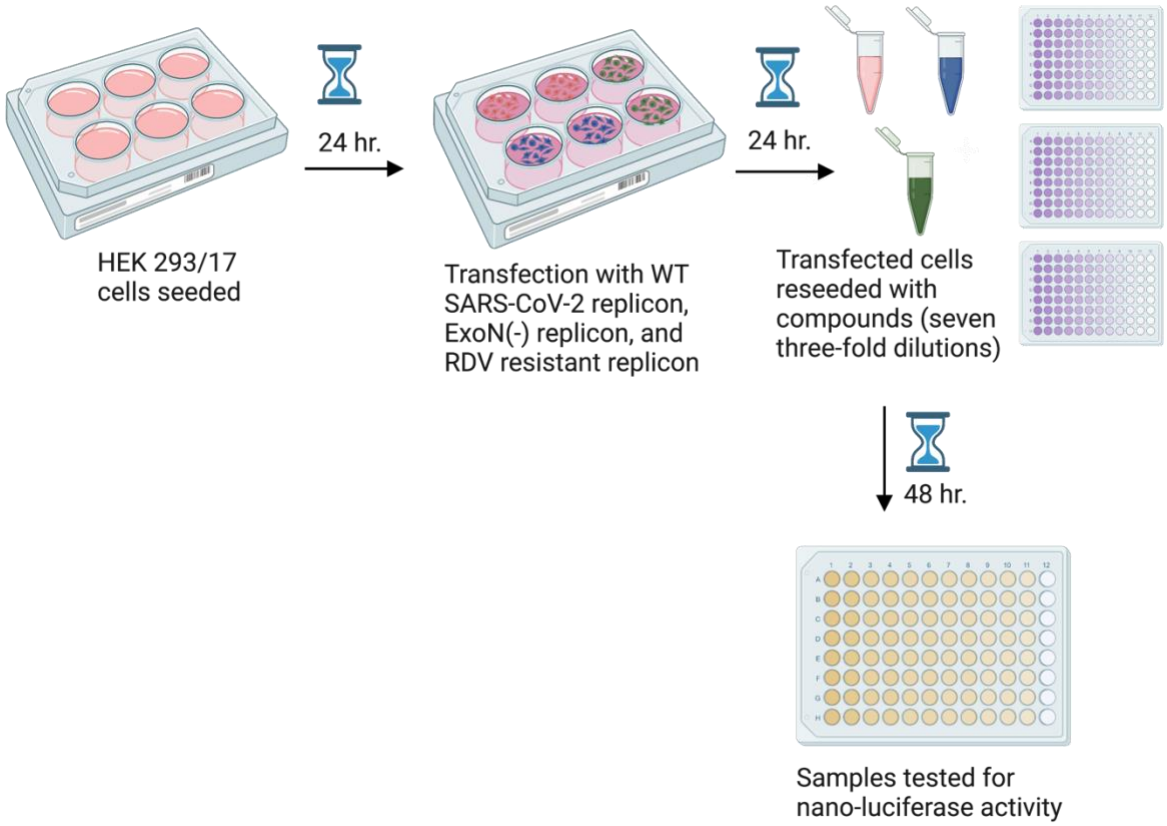

Figure 2.2 Luciferase assay for HEK 293T-17 cells with RdRp antiviral compounds 293T-17 cells were transfected with WT SARS-CoV-2, ExoN(-), and RDV-resistant replicons before incubation with novel RdRp antiviral compounds (RDRP-4 and RdRp-2). Red cells indicate transfection with WT SARS-CoV-2 replicon. Blue cells indicate transfection with ExoN(-) SARS-CoV-2 replicon. Green cells indicate transfection with RDV-resistant SARS-CoV-2 replicon.

2.5: Novel PLpro Targeting Antiviral Efficacy of Compounds

293T-17 cultured cells were tested for nanoluciferase activity following transfection with WT SARS-CoV-2 replicon and incubation with Kovari compounds using the methods described above. Stock solutions of Kovari compounds were made at a concentration of 20 μM in DMEM,

then mixed 1:1 with trypsinized transfected cells for a concentration of 10 µM on final plating. Luciferase activity was determined at a single concentration of 10 µM.

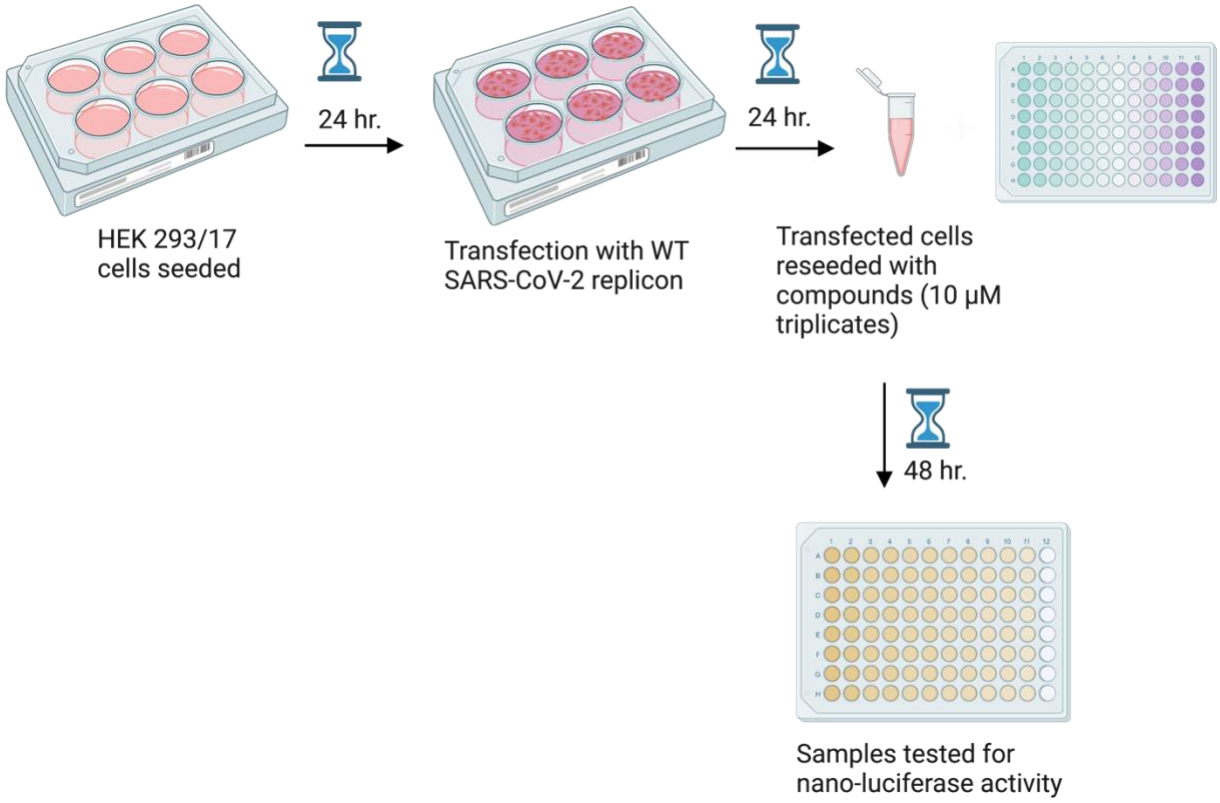

Figure 2.3 Luciferase assay for HEK 293T-17 cells with Kovari PLpro antiviral compounds

293T-17 cells were transfected with WT SARS-CoV-2 replicons before incubation with novel PLpro antiviral compounds (PL-0, PL-1, PL-2, PL-3, PL-4, PL-5, PL-6, PL-7, PL-8 and PL-9) at a single dose concentration. Red cells indicate transfection with WT SARS-CoV-2 replicon.

To determine antiviral efficacy of Progenra compounds in 293T-SARS-2R_GFP_NeoR_NL cells, the antiviral compounds (PR-1, PR-2, PR-3, PR-4, PR-5, PR-6, PR-7, PR-8) the methods described above were used again. Stock solutions of Progenra compounds were made at a concentration of 30 µM in DMEM, then mixed 1:1 with trypsinized transfected cells for a

concentration of 15 µM on final plating. Luciferase activity was determined at a single concentration of 15 µM. Cells treated with 0.15% DMSO were the negative control. 293T-SARS-2R_GFP_NeoR_NL cells were directly added to compounds (2 x 10^4 cells/well) without transfection with replicon.

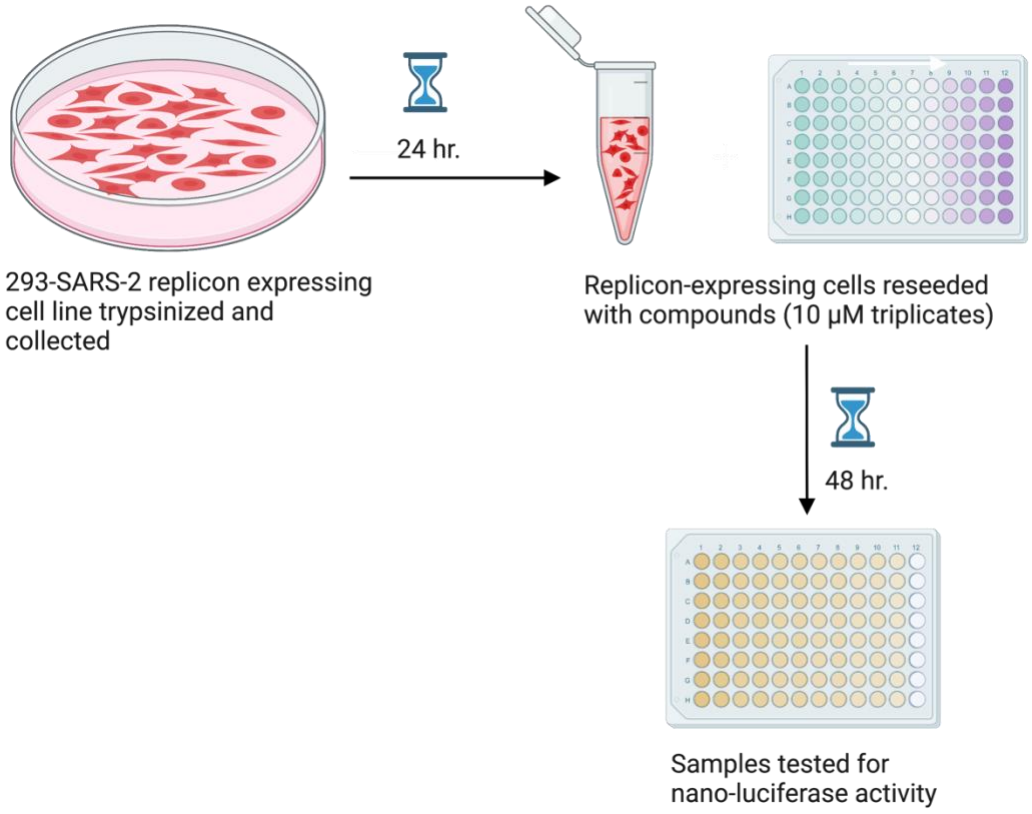

Figure 2.4 Luciferase assay for 293T-SARS-2R_GFP_NeoR_NL cells with Progenra PLpro antiviral compounds 293T-SARS-2R_GFP_NeoR_NL cells were incubated with novel PLpro antiviral compounds (PR-1, PR-2, PR-3, PR-4, PR-5, PR-6, PR-7, PR-8) at a single dose concentration.

2.6: Novel PLpro Targeting Experimental Antiviral Activity Assay (EC_{50})

To study dose-response effects, Kovari compounds PL-2, PL-3, PL-6, and PL-9 were screened in 293T-17 cells transfected with WT replicons and Progenra compounds PR-1, PR-2, PR-3, PR-7, and PR-8 were screened in 293T-SARS-2R_GFP_NeoR_NL cells using the protocol described in Methods Section 2.4. Kovari and Progenra compounds were prepared at a concentration of 60 μM in DMEM, then mixed 1:1 in 96-well plates with trypsinized transfected cells for a high concentration of 30 μM on final plating. DMSO-treated cells with 0.3% DMSO acted as a negative control.

2.7: PLpro Reporter Plasmid Construction and Screening

Lentiviral plasmids encoding for SARS-CoV-2 3CLpro (wild-type or C145A) and the Small BiT- cleavage-Large BiT-GFP reporter cassette were gifts from Wei-Shau Hu [44]. The Small BiT (SmBiT) and Large BiT (LgBiT) proteins allow for luciferase signaling when they are close to each other. Upon cleavage at the cleavage site separating these two proteins, the SmBit and LgBit disassociate preventing luciferase signaling.

To create a functional PLpro reporter vector, the 3CLpro sequence was replaced with wild-type PLpro amino acid sequence (catalytic triad Cys111, His 272, and Asp286 highlighted in green):

QVS-
GSISGEFAATMEVRTIKVFTTVDNINLHTQVVDMSMTYGQQFGPTYLDGADVTKIKPHN
SHEGKTFYVLPNDDTLRVEAFEYYHTTDPSFLGRYMSALNHTKKWKYPQVNGLTSIKW
ADNNCYLATALLTLQQIELKFNPPALQDAYYRARAGEAANFCALILAYCNKTVGELGD
VRETMSYLFQHANLDSCKRVLNVVCKTCGQQQTTLKGVEAVMYMGTLSYEQFKKGV
QIPCTCGKQATKYLVQQESPFVMMSAPPAQYELKHGTFTCASEYTGNYQCGHYKHITS
KETLYCDGALLTKSSEYKGPITDVFYKENSYTTTIKPVTYGSGATNFSLLKQAGDVEEN
PGPMHVTGYRLFEE

Or C111A PLpro amino acid sequence (yellow highlight indicates C111A inserted mutation):

QVS-
GSISGEFAATMEVRTIKVFTTVDNINLHTQVVDMSMTYGQQFGPTYLDGADVTKIKPHN
SHEGKTFYVLPNDDTLRVEAFEYYHTTDPSFLGRYMSALNHTKKWKYPQVNGLTSIKW
ADNNAYLATALLTLQQIELKFNPPALQDAYYRARAGEAANFCALILAYCNKTVGELGD
VRETMSYLFQHANLDSCKRVLNVVCKTCGQQQTTLKGVEAVMYMGTLSYEQFKKGV
QIPCTCGKQATKYLVQQESPFVMMSAPPAQYELKHGTFTCASEYTGNYQCGHYKHITS
KETLYCIDGALLTKSSEYKGPITDVFYKENSYTTTIKPVTYGSGATNFSLLKQAGDVEEN
PGPMHVTGYRLFEE

The 3CLpro nsp4/nsp5 cleavage site was replaced with one of three cleavage sites of PLpro framed by Smbit and Lgbit-GFP:

nsp1/nsp2 cleavage site sequence:
GACGTGGAGGAGAACCCTGGACCTATGCATGTGACCGGCTACCGGCTGTTCGAGGA
GATCCTGGGAGGTGGTTCTGGTGGTGGTTCAGGAGGCGGATCAAGGGAATTGAACG
GAGGAGCCTACACGCGGTATGTTATTCTCGGTGGAGGTTCTGGTGGAGGGAGCGGT
GGCGGGGGAGGTAGCGGCGGAGGGTCAGGCGGCGGCT

nsp2/nsp3 cleavage site sequence:
GACGTGGAGGAGAACCCTGGACCTATGCATGTGACCGGCTACCGGCTGTTCGAGGA
GATTCTGGGTGGCGGGTCCGGAGGTGGGTCTGGTGGAGGCTCTTTTACACTTAAGGG
CGGAGCACCCACCAAGGTAACAATACTGGGAGGGGGTAGTGGGGGCGGAAGTGGC
GGGGGCGGCGGCAGCGGCGGTGGCTCCGGAGGCGGCT

nsp3/nsp4 cleavage site sequence:
GACGTGGAGGAGAACCCTGGACCTATGCATGTGACCGGCTACCGGCTGTTCGAGGA
GATTTTGGGGGGAGGATCCGGTGGAGGTAGCGGAGGCGGTTCAATTGCCCTTAAGG
GCGGAAAAATCGTCAACAACTGGATCCTCGGGGGGGGAAGCGGAGGTGGTTCCGGG
GGAGGCGGTGGTAGTGGCGGAGGGTCAGGTGGCGGCT

The 3CLpro plasmid was linearized with digestive enzymes XbaI and EcoRI to remove 3CLpro and the reporter cassette consisting of SmBiT and unique 3CLpro cleavage site. Afterwards, gel-extraction techniques were used to purify it. An NEBuilder HiFi DNA Assembly reaction was performed with the extracted 3CLpro linearized plasmid, mutated or wild-type PLpro sequence and one of the three cleavage site sequences. The constructed PLpro reporter plasmids were then transformed into NEB 5-alpha competent E. coli cells (C2987 cells). Clones

were picked from the plate, grown and plasmid recovered by miniprep. Insertion of the PLpro and cleavage site sequences were confirmed by restriction digest with EcoRI and XbaI and gel electrophoresis. Clones with the correct size insertions were sent for Sanger Sequencing for sequence confirmation.

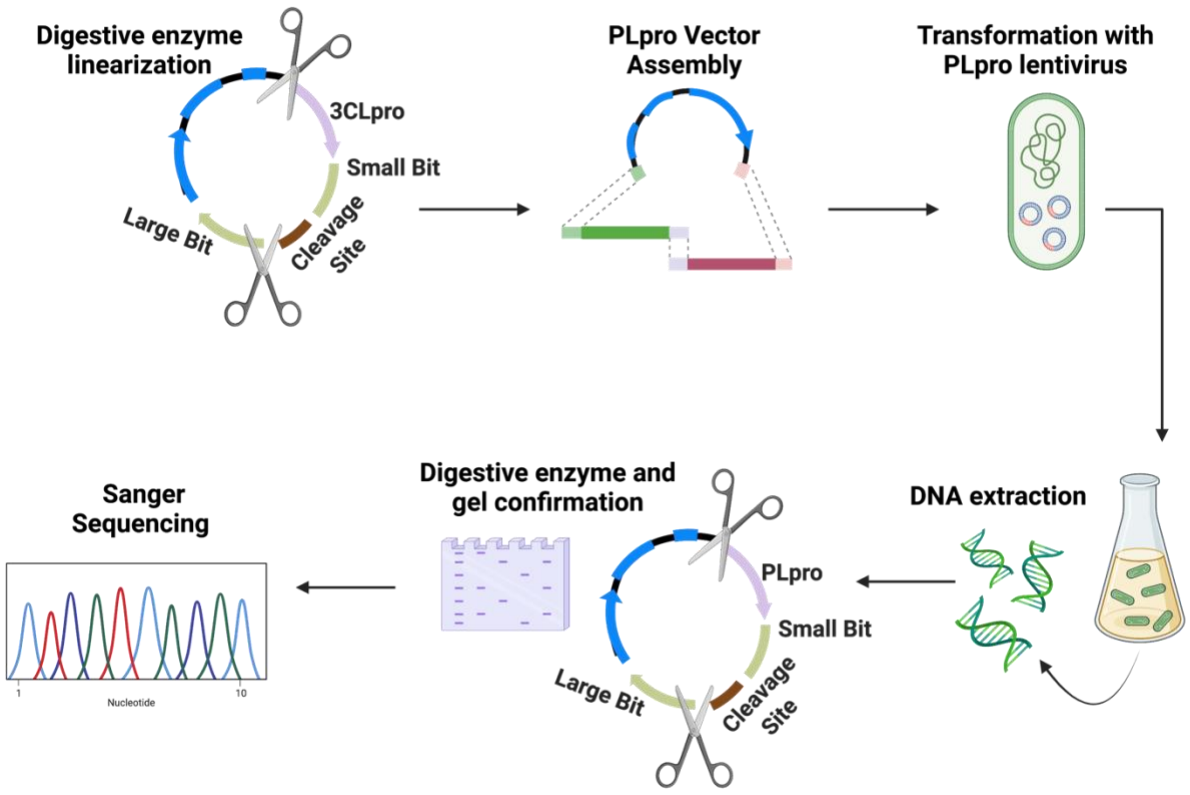

Figure 2.5 DNA Recombination Techniques for PLpro Plasmid Design. Assembly and restriction enzyme cleavage techniques used to assemble PLpro reporter plasmids from 3CLpro plasmids. Each PLpro plasmid contains one unique cleavage site (nsp 1/2, nsp 2/3, or nsp 3/4 cleavage sites included). Both WT and C111A PLpro plasmids were constructed.

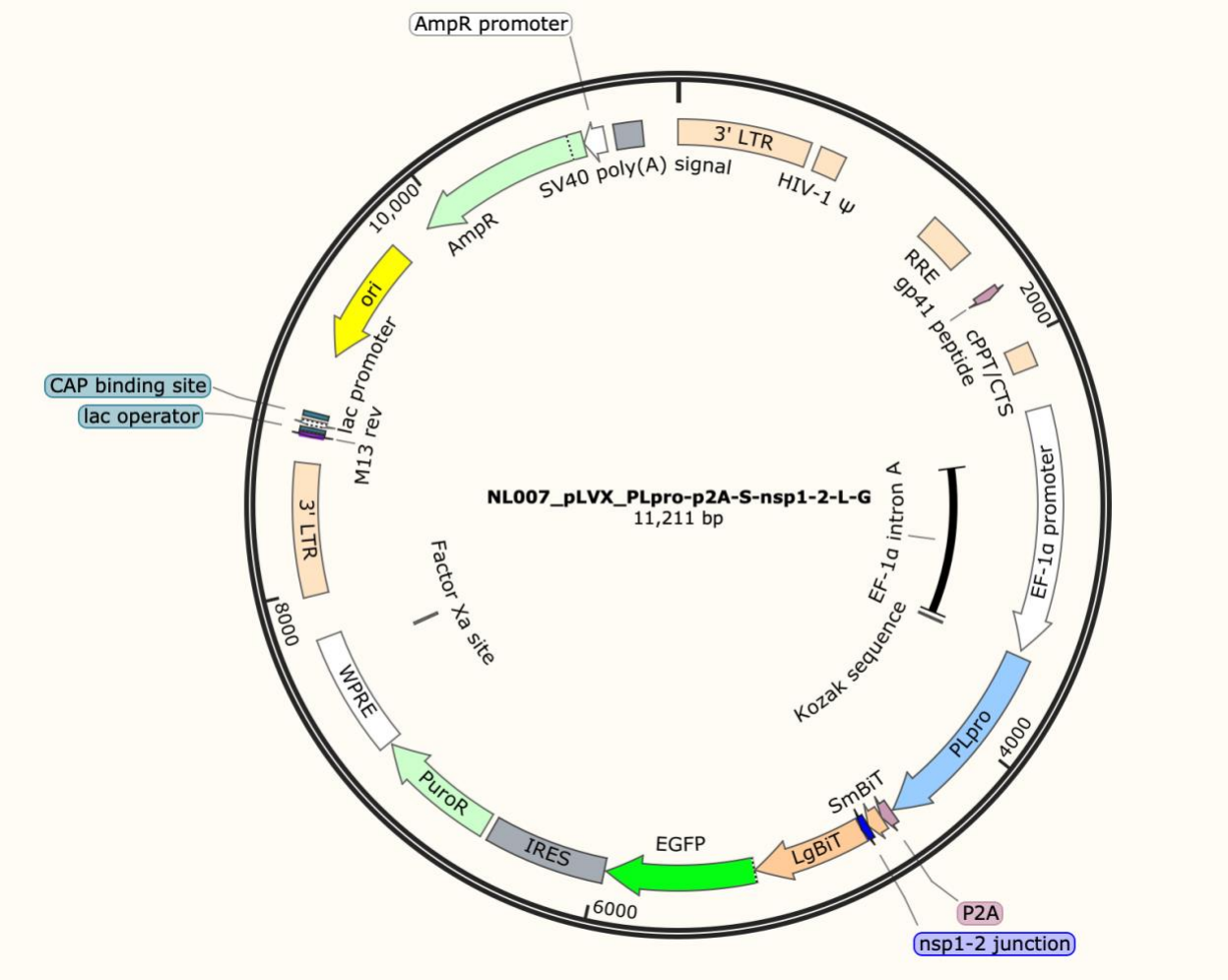

Figure 2.6 Constructed pLVX_PLpro-p2A-S-nsp1-2-L-G Plasmid. The Snapgene construct includes the pLVX-Puro HIV-1 based lentivirus vector with various genes, promoters, regulatory elements, and sequences that promote gene expression and viral packaging. Each plasmid consists of an inserted WT or C111A PLpro sequence and PLpro cleavage site.

To test PLpro vector inhibition by novel compounds and compare WT against C111A PLpro cell-based luciferase signaling, compounds PL-9, PR-1 and PR-8 were screened in 293T/17 cells transfected with constructed PLpro vectors. 293T/17 cells were seeded in 6-well plates (1.2×10^6 cells/well). After 24 hours, the PLpro WT and C111A vectors with inserted nsp3/4 cleavage sites

were transfected into 293T/17 cells using 2 µg PLpro plasmid/well, 200 µL/well Opti-MEM I Reduced Serum Medium (ThermoFisher), and 6 µL/well X-tremeGENE HP transfection reagent (Sigma-Aldrich). 24 hours following transfection, cells were washed with DPBS and removed from 6-well plates by trypsinization. Transfected cells were then pelleted and resuspended in DMEM at a concentration of (8×10^5 cells/mL). Stock solutions of PL-9, PR-1 and PR-8 were made at a concentration of 40 µM, 80 µM, and 80 µM respectively in DMEM, then mixed 1:1 in 96-well plates with trypsinized transfected cells for a high concentration of 20 µM, 40 µM, and 40 µM respectively on final plating. Three three-fold dilutions with three replicates per dilution were performed for all compounds. Media with 0.2% DMSO was used as a negative control. Luciferase activity was measured 48 hours after compound addition.

2.8: Statistical Analyses

Statistical analyses were performed in GraphPad Prism v9.3.1 (GraphPad Software, San Diego, CA, USA). Averaged data from each individual experiments was analyzed using a one-way ANOVA to determine p values.

3. Results

3.1: RdRp Dose-Response Antiviral Activity Assay (EC50)

To determine which antiviral RdRp-targeting compound had the highest potency we tested them against a SARS-CoV-2 replicon. The concentrations of the compounds encompassed a range from 40 µM to 0.055 µM. We found that RDRP-4 and RdRp-2 had lower EC_{50} values, and therefore higher inhibition, among all four compounds (Figure 3.1B). RdRp-2 was the most potent with an EC_{50} of 1.72 µM in WT replicons (Figure 3.1A).

In addition to potency, the utility of novel compounds may be enhanced if it can avoid resistance mechanisms that affect current standard of care. The nsp14 ExoN activity has been reporter to confer some protection against inhibition by RDV in a related coronavirus (MHV), presumably by excising incorporated RDV [32]. To determine whether ExoN played a role in SARS-CoV-2 sensitivity to these novel compounds, we used replicons with inactive ExoN. Our data showed that, except for RdRp-3, there was not a significant difference in EC_{50} values among the novel nucleoside analogue compounds and RDV (Figure 3.1.B). RdRp-3 had a four-fold higher EC_{50} value in WT SARS-CoV-2 in comparison to ExoN(-) SARS-CoV-2 across all three trials.

A.

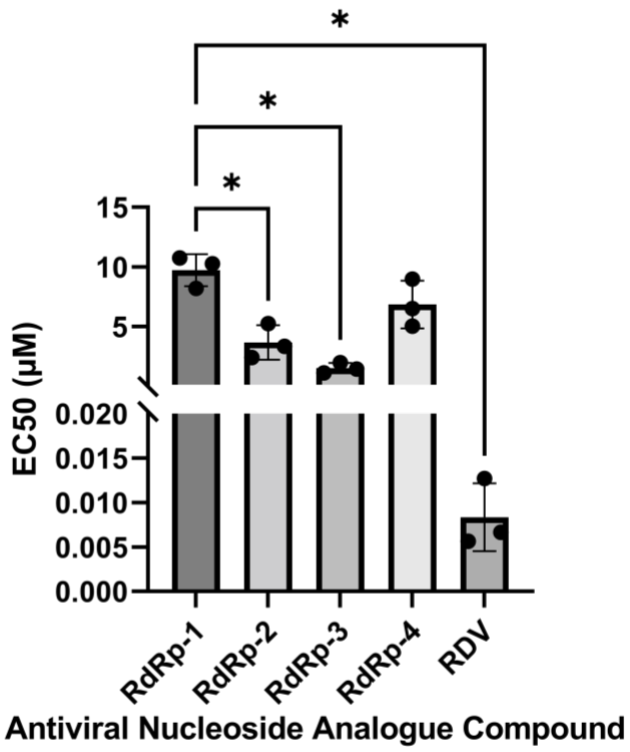

B.

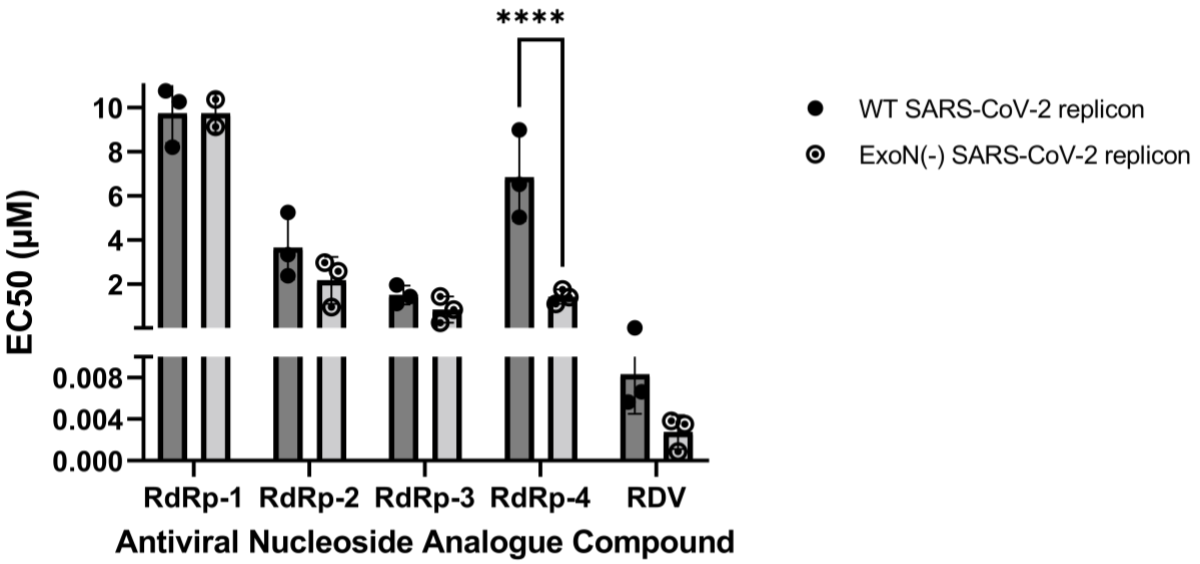

Figure 3.1 RdRp-targeting nucleoside analogue inhibition of SARS-CoV-2 replicons transfected with 293T-17 cells. 293T-17 cells were transfected with replicon, then reseeded in 96 well plates and treated with serially diluted nucleoside analogues. NLuc activity was measured 48 h post drug treatment. Error bars represent standard deviation.

A. EC_{50} values of compounds indicated in WT SARS-CoV-2 replicon. Means for EC_{50} shown. N=3. P value determined by one-way ANOVA. * $p<0.05$

B. EC_{50} values of compounds indicated in WT and ExoN(-) SARS-CoV-2 replicon. Means for EC_{50} shown. N=3. P value determined by one-way ANOVA. **** $p<0.0001$

We chose to examine the antiviral activity of compounds RDRP-4 and RdRp-2 in greater detail due to their low EC50 values in comparison to compounds RDRP-1 and RdRp-3. In WT replicons, RDRP-4 and RdRp-2 respectively had a statistically significant two-fold and six-fold decrease in EC50 values in comparison to compound RdRp-1 (Table 1). Therefore, these two compounds were screened with WT, ExoN(-), and RDV-resistant replicons. Four trials were

completed, however, only two trials provided calculatable EC50 values. The two trials not included in Table 1 had extreme variability between replicates and high percentage inhibition values across all concentrations of the compounds.

The data collected for compound testing of RDV and RDRP-4 (n=2) along with RdRp-2 (n-1) did not show any statistically significant differences in the EC50 values across all trials (Table 1). The ExoN(-) replicon had a higher resistivity to RDV than the RDV-resistant replicon by almost a two-fold difference (Table 1). Furthermore, the ExoN(-) replicon had a reduced sensitivity to RDRP-4 than WT and ExoN(-) replicon. Compound RdRp-2 screening in RDV-resistant replicons resulted in inconclusive EC50 values across all trials (Table 1). However, RdRp-2 has greater than a four-fold decrease in EC50 values from ExoN(-) to WT replicons (Table 1). More trials need to be completed to confirm the higher EC50 values seen in ExoN(-) replicon screening trials.

Table 1 Half-maximal effective values (EC_{50}) of RdRp-targeting nucleoside analogue in 293T-17 cells transfected with SARS-CoV-2 replicons. 293T-17 cells were transfected with replicon, then reseeded in 96 well plates and treated with serially diluted nucleoside analogues. NLuc activity was measured 48 h post drug treatment. $p = 0.7222$

293T-17 transfected cells with SARS-CoV-2 EC50 values (μM)	WT replicon	ExoN(-) replicon	RDV-resistant replicon
RDV (n=2)	0.00547 ± 0.000877	0.0284 ± 0.0321	0.0185 ± 0.0139
RdRp-2 (n=1)	0.216	0.966	-
RDRP-4 (n=2)	2.62 ± 2.86	8.11 ± 1.39	3.24 ± 4.23

3.2: Initial Screening of PLpro-Targeting Antiviral Compounds

To determine which Kovari Lab compound had the highest inhibitory effects on WT-SARS-CoV-2 replicons percent inhibition was first calculated for the novel compounds. All compounds were screened at 10 μM to identify those with significant antiviral properties that should be further tested in a dose-response manner. Similarly, Progenra company compounds, PR-1, PR-2, PR-3, PR-4, PR-5, PR-6, PR-7, PR-8, were tested at a single dose concentration of 15 μM. Only compounds that showed significant inhibitory potential at this concentration would be valuable to study in greater detail. RDV was used as a positive control and had a concentration of 0.1 μM in trials with Kovari compounds or 0.3 μM in trials with Progenra compounds.

PL-9 demonstrated the highest percentage inhibition in comparison to all novel Kovari compounds and RDV, reaching an almost 100% inhibition (Table 2). Furthermore, PL-9 had very low standard deviation between the two trials completed (Table 2). PL-2 had the second-highest inhibitory percentage followed by PL-6 and PL-3 (Table 2).

Analyses of each novel compound against DMSO-treated cells (negative control), revealed that four compounds induced significant inhibition. PL-2, PL-3, and PL-6 had an intermediate increase in percentage inhibition from the DMSO baseline ($p<0.005$) (Table 2). PL-9 showed even higher increases in percentage inhibition from baseline DMSO values ($p<0.001$) (Table 2).

Across the single-dose Progenra trials, PR-1, PR-2, PR-3, PR-7 and PR-8 demonstrated the highest percentage inhibitions (Table 3). PR-1 and PR-2 were especially inhibitory with a percentage of 93% and 91% respectively (Table 3).

Analysis of the percentage inhibition data compared to DMSO revealed that compounds PR-1, PR-2, PR-3, PR-7 and PR-8 had statistically significant inhibition ($p<0.005$) (Table 3). PR-5 had slightly greater inhibition than DMSO baseline cells ($p<0.05$) as well (Table 3). The

novel compounds and RDV did not have statistically significant differences in percentage inhibition when compared to each other (Table 3).

Table 2: WT SARS-CoV-2 replicon single-dose (10 μM) percentage inhibition values. 293T-17 cells were transfected with replicon, then reseeded in 96 well plates and treated with single-dose PLpro-targeting compounds. NLuc activity was measured 48 h post drug treatment. A one-way ANOVA test across all compounds and DMSO-treated cells resulted in $p<0.0001$. N=2.

Transfected 293T-17 cells with WT SARS-CoV-2 replicon	Trial 1	Trial 2	Averages ± Stdev
RDV	91.7%	90.8%	91.2 ± 2.01%
PL-0	-11.2%	-48.4%	-29.8 ± 25.07 %
PL-1	50%	27.5%	38.7± 12.8%
PL-2	93.9%	92.5%	93.2 ± 1.98%
PL-3	89.1%	80.4%	84.7 ± 5.02%
PL-4	64.2%	57.0%	60.6 ± 9.28%
PL-5	33.9%	17.1%	17.8 ± 30.4%
PL-6	88.5%	84.9%	86.7± 4.97%
PL-7	52.5%	35.5%	44.0 ± 16.3%
PL-8	65.4%	53.8%	59.6 ± 6.96%
PL-9	99%	99%	99.0 ± 0.226%

Table 3: 293T-SARS-2R_GFP_NeoR_NL single-dose (15 μM) percentage inhibition values. 293T-SARS-2R_GFP_NeoR_NL were reseeded in 96 well plates and treated with single-dose PLpro-targeting compounds. NLuc activity was measured 48 h post drug treatment A one-way ANOVA test across all compounds and DMSO-treated cells resulted in $p=0.0009$. N=2.

293T-SARS-2R_GFP_NeoR_NL cells	**Trial 1**	**Trial 2**	**Averages± Stdev**
RDV	93.4%	93.8%	94.3 ± 7.30%

PR-1 (small molecule)	97.4%	89.3%	93.4 ± 11.1%
PR-2 (Small molecule PROTAC ligand)	89.3%	92.8%	91.1 ± 8.00%
PR-3 (PROTAC)	70.8%	99.1%	85.0 ± 21.1%
PR-4 (Small molecule)	65.3%	24.8%	45.9 ± 19.5%
PR-5 (PROTAC)	86.6%	53.6%	78.3 ± 18.6%
PR-6 (PROTAC)	45.7%	56.7%	48.5 ± 40.1%
PR-7 (PROTAC)	76.6%	86.8%	78.3 ± 14.1%
PR-8 (PROTAC)	84.1%	98.0%	89.5 ± 15.2%

3.3: PLpro-Targeting Dose-Response Antiviral Activity Assay (EC50)

PL-2, PL-3, PL-6 and PL-9 showed the highest percent inhibition values and were chosen for further analysis. We tested the Kovari compounds at seven different concentrations ranging from 30 μM to 0.04 μM (three-fold dilutions) to determine EC_{50}. At this concentration range, compound PL-9 did not fall below 50%. Therefore, we re-tested this compound in three more trials with a concentration range of 0.33 μM to 0.000453 (seven three-fold dilutions).

We found that, like the results seen in single-dose analyses of the Kovari compounds, PL-9 had the greatest inhibitory effects among all compounds (EC_{50} = 0.0782 μM) (Figure 3.2). PL-9 had a 100-fold lower EC50 value than PL-2 and greater than a 100-fold lower EC50 value than PL-3 and PL-6 (Figure 3.2). PL-3 and PL-6 do not have statistically significant difference in inhibition and have higher EC50 values than both PL-2 and PL-9 (Figure 3.2). Therefore, results

from the dose-response analysis confirmed single-dose percent inhibition for the novel Kovari compounds tested.

PR-1, PR-2, PR-3, PR-7 and PR-8 were all chosen for further inhibition analysis due to their inhibition in single dose experiments. PR-1 and PR-2 demonstrated the lowest EC50 values in accordance with their high percentage inhibition in previous experimentation (Table 3). PROTAC PR-8 also demonstrated the lowest EC50 value (0.616 μM) out of all the PROTACs (Table 3). PR-7 produced only a single conclusive EC50 value across three trials. Statistical analyses of the data showed no statistically significant differences in EC50 and therefore inhibition between the compounds

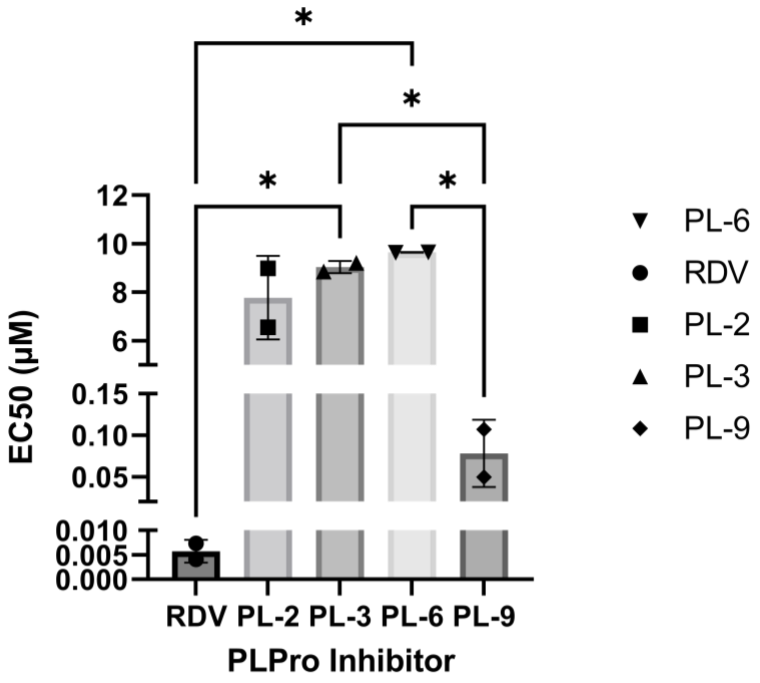

Figure 3.2 PLpro-targeting small molecule and PROTAC inhibitors of 293T-SARS-2R_GFP_NeoR_NL cells. Graph of WT SARS-CoV-2 replicon half-maximal drug response after incubation with indicated compounds. All compounds were tested in a dose-response

manner. PL-9 had a high concentration of 0.33 μM while compounds PL-2, PL-3, and PL-6 started at a high concentration of 30 μM. A one-way ANOVA test across all compounds and DMSO-treated cells resulted in p=0.0698.

Table 3: WT SARS-CoV-2 replicon half-maximal drug response after incubation with indicated compounds. All compounds were tested in a dose-response manner. N=2. A one-way ANOVA test across all compounds and DMSO-treated cells resulted in p= 0.3583, no significance.

293T-SARS-2R_GFP_NeoR_NL cells EC50 (μM)	**Averages ± Stdev**
RDV	0.0044 ± 0.0062 (n=3)
PR-1 (small molecule)	0.091± 0.10 (n=3)
PR-2 (Small molecule PROTAC ligand)	1.3 ± 1.3 (n=3)
PR-3 (PROTAC)	130 ± 180 (n=2)
PR-7 (PROTAC)	1.2 (n=1)
PR-8 (PROTAC)	0.62 ± 0.032 (n=2)

3.4: Validation and Testing of Novel PLPro Reporter Assay

One limitation of replicons for compound screening is that we cannot know for sure which of the essential viral processes is being inhibited. To facilitate validation and mechanistic studies of putative PLpro inhibitors, we generated a cell-based PLpro assay, based on the approach of the Wei-Shau Hu Lab's development of a 3CLpro reporter vector [44]. The 3CLpro sequence was replaced with a PLpro sequence and 3CLpro-specific cleavage sites were replaced with PLpro-specific cleavage sites. As a positive control for inhibition of the viral protease, we produced an enzymatically dead mutant in with a C111A mutation in the PLPro sequence.

We were able to confirm the success of the PLpro reporter assay assembly through digestive enzyme and purification methods along with Sanger sequencing. Following confirmation, the

PLpro reporter vector was tested with compounds PL-9, PR-1 and PR-8. These three compounds are all PLpro-inhibitors and demonstrated high inhibitory efficacy in previous experimentation.

Initial comparison of the WT and enzymatically dead PLPro reporter assay revealed three-fold higher NanoBiT activity of the C111A vector in comparison to WT vector (Figure 3.3). C111A PLpro vectors maintained relatively high luciferase signaling (~6e+04 RLU) when incubated with lower than 20 μM concentrations of PL-9 and PR-1 (Figure 3.3). WT PLpro vectors maintained lower luciferase signaling in comparison to WT PLpro (~ 1.7e+04) when incubated with lower than 20 μM concentrations of PL-9 and PR-1 (Figure 3.3). We observed a ten-fold decrease in WT PLpro vector NanoBiT activity following an increase in PL-9 concentration from 6.67 μM to 20 μM (Figure 3.3A). The C111A PLpro vector also demonstrates a decrease in activity (five-fold) when PL-9 concentration increases (Figure 3.3A). Dose-response changes in nanoluciferase signaling were not observed in PLpro vectors incubated with PR-1 (Figure 3.3B).

A.

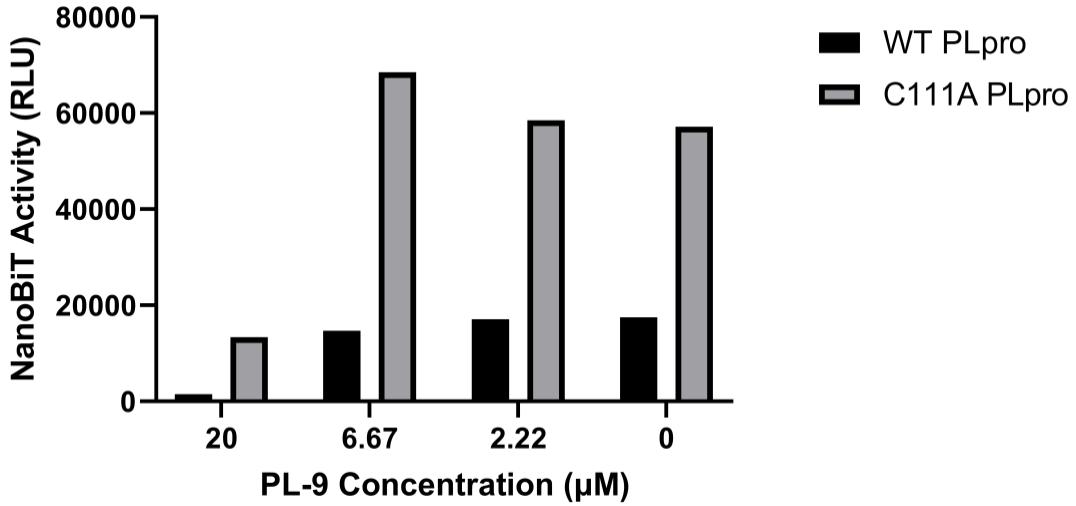

B.

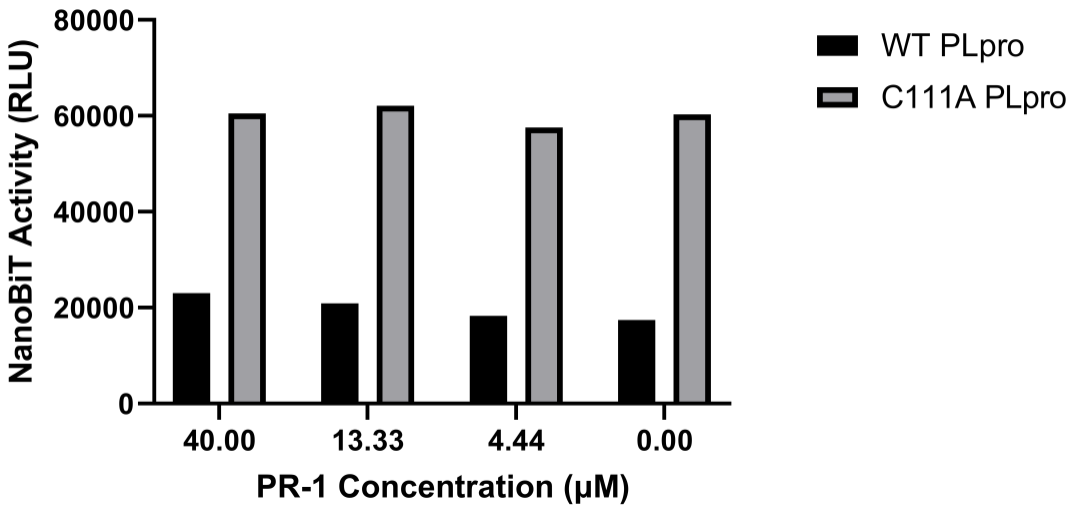

Figure 3.3 PLpro vector NanoBiT luciferase activity in transfected 293T-17 cells.

A. NanoBiT activity (relative luciferase units) measured following 48 hours of incubation with PL-9. All PLpro reporter vectors have a nsp3/4 cleavage site and either WT PLpro or C111A PLpro. (N=1).

B. NanoBiT activity (relative luciferase units) measured following 48 hours of incubation with PR-1. All PLpro reporter vectors have a nsp3/4 cleavage site and either WT PLpro or C111A PLpro. (N=1).

4. Discussion

Antiviral therapies are an essential tool in the ongoing fight against COVID-19. Their inhibitory effects against certain steps of the SARS-CoV-2 replication cycle make such compounds especially favorable as another tool to decrease death rates and hospitalizations. In this study I have examined 21 novel antiviral compounds against SARS-CoV-2 and identified 9 compounds with promising inhibitory effects, including 3 with submicromolar potency.

In my first screening of RdRp-targeting nucleoside analogue compounds, both RdRp-2 and RDRP-4 showed lower EC_{50} than RDRP-1 in WT SARS-CoV-2. Exonuclease has been proposed to increase viral resistance to nucleoside analogues such as RDV and the novel RdRp-targeting compounds due to its excision-based proofreading activity. Screening of the novel compounds with ExoN(-) replicons confirmed that RS-39995a and RDRP-4 have higher inhibitory effects than RDRP-1. Furthermore, ExoN(-) SARS-CoV-2 did not demonstrate resistance to RDRP-1, RDRP-4, and RdRp-2 inhibition. While RDV had slightly greater EC50 values in ExoN(-) replicons the difference was not statistically significant. These results contrast to the studied resistance of ExoN(-) MHV to RDV in live virus experimentation. More studies need to be completed before concluding that SARS-CoV-2 ExoN activity does not decrease nucleoside analogue inhibitory drug effects. More replicates will help decrease the inter-replicate variability observed in the data. Such variability could be due to differences in transfection efficiency and pipetting errors. To decrease the variation that could result from inconsistent transfected DNA per sample, we recommend scanning for green fluorescent protein (GFP) to determine transfected gene expression before compound incubation. Since RDV also did not show significant differences between the two replicons, we cannot extrapolate that RDRP-1, RDRP-4 and RdRp-2 are not recognized and excised by Coronavirus ExoN enzymes.

Previous live viral studies on MHV showed increased sensitivity to the active-form of RDV in ExoN(-) viruses (4.5 fold-decrease from 0.087μM to 0.019 μM) [32]. Our data on SARS-CoV-2 WT and ExoN(-) replicons did not demonstrate such decreased sensitivities to RDV, RDRP-1, RDRP-4, or RdRp-2. The discrepancies between our study on SARS-CoV-2 and studies with MHV could be due to our use of a replicon-system for in vitro screening. Furthermore, these differences could be due to variances between drug potency and inhibitory

potentials in SARS-CoV-2 and MHV. Future screening of these compounds with live virus in cell culture experimentation can reveal exonuclease activity in physiological conditions.

RdRp-3 was more potent in ExoN(-) SARS-CoV-2 replicons than WT SARS-CoV-2 replicons. We predict that exonuclease activity in the WT replicon led to excision of RdRp-3 and increased the resistance of WT SARS-CoV-2 against this compound.

Screening of RdRp-2 and RDRP-4, with an additional RDV-resistant replicon let to inconclusive EC_{50} values. Although four trials were completed for these compounds, half failed to result in viable EC_{50}. Our inhibitory percentages were highly variable across all concentrations and did not show the dose-response differences demonstrated in previous trials. We suspect that such inconclusive results could stem from low cell viability and therefore luciferase signaling. The variability in our data could also stem from cell clumping resulting in extremely high luciferase signaling for several samples. Across the trials that did produce conclusive EC_{50} values, the ExoN(-) replicon had less sensitivity to all three screened compounds in comparison to WT and RDV-resistant replicons. Such data directly opposes the results of the MHV ExoN(-) study. Our results showed that the RDV-resistant replicon had a 3.34-fold increase in resistance which is similar to the 5.6-fold increase in resistance seen in live MHV from WT to RDV-resistant virus. Such increases in resistance are not seen in the screening with RdRp-2 and RDRP-4. Therefore, we conclude that the RDV-resistance mutations in our replicon are specific to RDV and are not ubiquitous. None of the Schinazi compounds produced sub-micromolar EC_{50} values and cannot be considered hits in comparison to known RdRp inhibitors such as RDV and Molnupiravir.

Out of the ten Kovari Lab PLpro-targeting compounds screened, four produced significant inhibition in WT SARS-CoV-2 and were selected for further screening (PL-2, PL-3,

PL-6 and PL-9). Secondary screening of these compounds showed that compound PL-9 is the most potent novel antiviral compound tested out of all Kovari Lab, Schinazi Lab and Progenra Company compounds tested. PL-9 had an EC50 value of 0.0782 μM and showed a statistically significant decrease in EC50 in comparison to PL-3 and PL-6. In comparison to the known PLpro inhibitor, GRL0617 (EC_{50} = 2.1 μM in HEK293T cells transfected with PLpro-encoding plasmids), PL-9 appears have greater potency [46]. More dose-response antiviral activity assay trials along with cell cytotoxicity trials with PL-9 can confirm whether PL-9 enzymatically inhibits PLpro or if its studied inhibitory effects are due to confounding variables such as cell cytotoxicity.

Our screening of eight Progenra company compounds resulted in five promising compounds (PR-1 (small molecule), PR-2 (small molecule ligand), PR-3 (small molecule PROTAC ligand), PR-7 (PROTAC), and PR-8 (PROTAC)). The secondary dose-response screening of these compounds confirmed the studied differences in drug percent inhibitions. All the compounds that resulted in higher inhibition than PR-4, PR-5, and PR-6 have covalent binding capabilities. PR-4, PR-5, and PR-6 inhibit through noncovalent binding which we have found decreases inhibitory potential. This is in accordance with previous data about the advantages of covalent inhibitors due to their irreversible binding effects [47].

The small molecule inhibitor and small molecule PROTAC ligand (PR-1 and PR-2) both demonstrated higher inhibitory potential than the tested PROTACS. Out of the three screened PROTACs, PR-3 has the lowest inhibitory potential despite being developed from PR-1 and PR-2. The inhibition of PR-1 is suggestive that the inhibitory effects of PR-3 are due to inhibition of PLpro enzymatic activity rather than the degradation of PLpro via the proteosome-ubiquitin complex. As the original small molecule inhibitor PR-1 is converted to the PR-3 PROTAC,

inhibitory activity is lost. This could be due to the increased size of the PROTAC form and/or lower transmembrane solubility properties.

Furthermore, PROTACS PR-7 and PR-8 demonstrated lower inhibitory potential in the stable cell line. More trials can help determine whether the differences in the EC50 values of these compounds are statistically significant. Compound screening should also be completed in a different model system, such as live virus or cell-based luciferase assays, to confirm results. Creating a "BUMP" version of the PROTAC compounds could serve as a negative control and confirm the EC_{50} values determined. "BUMP" PROTACs have methylated glutarimide moieties that prevent E3 ligase binding, while maintaining the PROTAC structure [48].

Unpublished data from the Sarafianos Lab shows that in Calu-3 cells infected with SARS-CoV-2, PR-2 (EC_{50} = 6.1 μM) demonstrated a three-fold increase in EC_{50} values in comparison to PR-1 (EC_{50} = 2.3 μM) [49]. PR-3 had extremely low potency and its EC_{50} could not be calculated in this system [49]. Similarly, in our experiment we observed an EC_{50} increase from 0.09 μM to 1.30 μM between testing with PR-1 and PR-2 and very low PR-3 antiviral efficacy (EC_{50} = 126 μM). Therefore, across both live SARS-CoV-2 infected cell lines and stable cell lines expressing SARS-CoV-2 replicons there is a decrease in compound inhibition as PR-1 is modified to make PR-2 [49]. Further unpublished data from the Sarafianos Lab showed that in the stable SARS-CoV-2 replicon cell line only compounds PR-1 and PR-7 were cytotoxic at 30 μM (28.3% and 39.0% percentage viability respectively) [50]. The high cytotoxicity of these compounds at 30 μM could account in part for their low EC_{50} values [50]. Going forward, it will be necessary to monitor toxicity closely, to avoid confounding potency data. Further dose-response testing starting from a concentration of 10 μM should be completed to support the previously recorded EC_{50} data.

To further test antiviral compound hits, PL-9 and PR-1, a PLpro cell-based luciferase assay was used. PLpro reporter assay testing revealed that in non-inhibitory conditions the C111A PLpro vector has three-fold higher luciferase signaling. These results demonstrated that the negative control C111A vector has decreased protease activity as decreased cleavage of the SmBiT and LgBiT reporter cassette allows for luciferase activity. This negative control helps validate the PLpro activity of the WT assay that results in lower luciferase signaling. Dose-response differences in C111A and WT PLpro signaling were not observed indicating the low-sensitivity of this reporter assay to concentration changes. At 20 μM PL-9 we observed a significant decrease in luciferase activity of both C111A and WT PLpro vectors. We predict that this decrease in signaling is due to the cytotoxic effects of PL-9 rather than inhibition. PL-9-mediated inhibition of PLpro would have resulted in decreased reporter cassette cleavage and higher luciferase signaling which is the opposite of the observed effects. The decreased signaling of the C111A vector further confirms the possible cytotoxic effects of PL-9 at 20 μM concentration. A cytotoxic assay of PL-9 in 293T-17 cells transfected with PLpro vectors can help confirm these predictions. Furthermore, as only one cell-based luciferase assay trial was completed, more trials need to be carried out to determine the statistical significance of the results.

In the 3CLpro cell-based luciferase assay our PLpro reporter assay was based on, researchers observed a 9.6-fold increase between the WT and mutant vector [44]. Furthermore, both the WT and mutant 3CLpro constructs resulted in ten-fold higher NanoBiT activity than our PLpro reporter vector. The higher signaling abilities and greater difference in enzymatic activity between the WT and negative control 3Clpro vectors reveal that our PLpro assay is not as effective as the 3CLpro assay at screening antiviral compounds. The 3CLpro luciferase-

complementation assay was also able to accurately demonstrate concentration-dependent inhibition of SARS-CoV-2 3CLpro cleavage unlike our vector [44]. The dose-response capabilities of the 3CLpro vector were observed following incubation with a known 3CLpro antiviral compound GC376 [44]. We recommend further testing of our PLpro reporter vector with a known inhibitor of PLpro, such as GRL0617 (EC_{50} = 2.1 μM). This will confirm whether the absence of dose-response differences in PLpro signaling is due to low vector sensitivity or low novel drug compound inhibition. Since we studied the PLpro vector with only novel antiviral compounds, PL-9 and PR-1, GRL0617 will serve as a positive control.

In summary, we screened twenty-one novel SARS-CoV-2 inhibitory compounds for antiviral activity and found three hits (PL-9, PR-1 and PR-8). Out of these three compounds, PL-9 is the most promising. Although our experimentation was limited in terms of trial numbers and model biological systems, we were still able to determine the relative therapeutic potencies of the tested compounds. Furthermore, we examined the specific effects of four compounds on SARS-CoV-2 with knockout Exonuclease or RdRp to determine these proteins' impact on antiviral efficacies. Our research helped identify which compounds have promising antiviral activity and should be studied in greater detail along with compounds that have insignificant potency against SARS-CoV-2.

5. References

1. Katella, K. *Our Pandemic Year - A COVID-19 Timeline*. 2021.
2. WHO, *WHO Director-General's opening remarks at the media briefing on COVID-19 - 11 March 2020*. 2020.
3. WHO. *WHO COVID-19 Dashboard*. 2021.
4. Fehr, A.R. and S. Perlman, *Coronaviruses: an overview of their replication and pathogenesis.* Methods in molecular biology (Clifton, N.J.), 2015. **1282**: p. 1-23.
5. Snijder, E.J., E. Decroly, and J. Ziebuhr, *The Nonstructural Proteins Directing Coronavirus RNA Synthesis and Processing.* Adv Virus Res, 2016. **96**: p. 59-126.
6. Ortiz-Prado, E., et al., *Clinical, molecular, and epidemiological characterization of the SARS-CoV-2 virus and the Coronavirus Disease 2019 (COVID-19), a comprehensive literature review.* Diagnostic Microbiology and Infectious Disease, 2020. **98**(1): p. 115094.
7. Jiang, P., et al., *Picornavirus morphogenesis.* Microbiology and molecular biology reviews : MMBR, 2014. **78**(3): p. 418-437.
8. Gorbalenya, A.E., et al., *The species Severe acute respiratory syndrome-related coronavirus: classifying 2019-nCoV and naming it SARS-CoV-2.* Nature Microbiology, 2020. **5**(4): p. 536-544.
9. Petersen, E., et al., *Comparing SARS-CoV-2 with SARS-CoV and influenza pandemics.* The Lancet Infectious Diseases, 2020. **20**(9): p. e238-e244.
10. Salzberger, B., et al., *Epidemiology of SARS-CoV-2.* Infection, 2021. **49**(2): p. 233-239.
11. Elezkurtaj, S., et al., *Causes of death and comorbidities in hospitalized patients with COVID-19.* Scientific Reports, 2021. **11**(1): p. 4263.
12. Naqvi, A.A.T., et al., *Insights into SARS-CoV-2 genome, structure, evolution, pathogenesis and therapies: Structural genomics approach.* Biochimica et Biophysica Acta (BBA) - Molecular Basis of Disease, 2020. **1866**(10): p. 165878.
13. Kim, D., et al., *The Architecture of SARS-CoV-2 Transcriptome.* Cell, 2020. **181**(4): p. 914-921.e10.
14. Hu, B., et al., *Characteristics of SARS-CoV-2 and COVID-19.* Nature Reviews Microbiology, 2021. **19**(3): p. 141-154.
15. Tufan, A., A. Avanoğlu Güler, and M. Matucci-Cerinic, *COVID-19, immune system response, hyperinflammation and repurposing antirheumatic drugs.* Turkish journal of medical sciences, 2020. **50**(SI-1): p. 620-632.
16. Van Damme, W., et al., *The COVID-19 pandemic: diverse contexts; different epidemics-how and why?* BMJ global health, 2020. **5**(7): p. e003098.
17. Lauring, A.S. and P.N. Malani, *Variants of SARS-CoV-2.* JAMA, 2021. **326**(9): p. 880-880.
18. Harrison, A.G., T. Lin, and P. Wang, *Mechanisms of SARS-CoV-2 Transmission and Pathogenesis.* Trends in Immunology, 2020. **41**(12): p. 1100-1115.
19. Roe, M.K., et al., *Targeting novel structural and functional features of coronavirus protease nsp5 (3CLpro, Mpro) in the age of COVID-19.* Journal of General Virology, 2021. **102**(3).

20. V'kovski, P., et al., *Coronavirus biology and replication: implications for SARS-CoV-2.* Nature Reviews Microbiology, 2021. **19**(3): p. 155-170.
21. Ahidjo, B.A., et al., *Current Perspective of Antiviral Strategies against COVID-19.* ACS Infectious Diseases, 2020. **6**(7): p. 1624-1634.
22. Yadav, R., et al., *Role of Structural and Non-Structural Proteins and Therapeutic Targets of SARS-CoV-2 for COVID-19.* Cells, 2021. **10**(4): p. 821.
23. Osipiuk, J., et al., *Structure of papain-like protease from SARS-CoV-2 and its complexes with non-covalent inhibitors.* Nature Communications, 2021. **12**(1): p. 743.
24. McClain, C.B. and N. Vabret, *SARS-CoV-2: the many pros of targeting PLpro.* Signal Transduction and Targeted Therapy, 2020. **5**(1): p. 223.
25. Gao, X., et al., *Crystal structure of SARS-CoV-2 papain-like protease.* Acta Pharmaceutica Sinica B, 2021. **11**(1): p. 237-245.
26. Lei, J., Y. Kusov, and R. Hilgenfeld, *Nsp3 of coronaviruses: Structures and functions of a large multi-domain protein.* Antiviral research, 2018. **149**: p. 58-74.
27. Tahir, M., *Coronavirus genomic nsp14-ExoN, structure, role, mechanism, and potential application as a drug target.* Journal of Medical Virology, 2021. **93**(7): p. 4258-4264.
28. Minskaia, E., et al., *Discovery of an RNA virus 3'→5' exoribonuclease that is critically involved in coronavirus RNA synthesis.* Proceedings of the National Academy of Sciences of the United States of America, 2006. **103**(13): p. 5108-5113.
29. Zuo, Y. and M.P. Deutscher, *Exoribonuclease superfamilies: structural analysis and phylogenetic distribution.* Nucleic acids research, 2001. **29**(5): p. 1017-1026.
30. Ogando Natacha, S., et al., *The Enzymatic Activity of the nsp14 Exoribonuclease Is Critical for Replication of MERS-CoV and SARS-CoV-2.* Journal of Virology. **94**(23): p. e01246-20.
31. Bar-On, Y.M., et al., *Science Forum: SARS-CoV-2 (COVID-19) by the numbers.* elife, 2020. **9**: p. e57309.
32. Agostini, M.L., et al., *Coronavirus Susceptibility to the Antiviral Remdesivir (GS-5734) Is Mediated by the Viral Polymerase and the Proofreading Exoribonuclease.* mBio, 2018. **9**(2): p. e00221-18.
33. Pachetti, M., et al., *Emerging SARS-CoV-2 mutation hot spots include a novel RNA-dependent-RNA polymerase variant.* Journal of Translational Medicine, 2020. **18**(1): p. 179.
34. Jiang, Y., W. Yin, and H.E. Xu, *RNA-dependent RNA polymerase: Structure, mechanism, and drug discovery for COVID-19.* Biochemical and biophysical research communications, 2021. **538**: p. 47-53.
35. Noh, J.Y., H.W. Jeong, and E.-C. Shin, *SARS-CoV-2 mutations, vaccines, and immunity: implication of variants of concern.* Signal Transduction and Targeted Therapy, 2021. **6**(1): p. 203.
36. Tiwari, V., et al., *Discovering small-molecule therapeutics against SARS-CoV-2.* Drug discovery today, 2020. **25**(8): p. 1535-1544.
37. Shannon, A., et al., *Remdesivir and SARS-CoV-2: Structural requirements at both nsp12 RdRp and nsp14 Exonuclease active-sites.* Antiviral research, 2020. **178**: p. 104793-104793.
38. Chien, M., et al., *Nucleotide Analogues as Inhibitors of SARS-CoV-2 Polymerase, a Key Drug Target for COVID-19.* Journal of Proteome Research, 2020. **19**(11): p. 4690-4697.

39. Báez-Santos, Y.M., S.E. St John, and A.D. Mesecar, *The SARS-coronavirus papain-like protease: structure, function and inhibition by designed antiviral compounds.* Antiviral research, 2015. **115**: p. 21-38.
40. He, Y., et al., *Proteolysis targeting chimeras (PROTACs) are emerging therapeutics for hematologic malignancies.* Journal of Hematology & Oncology, 2020. **13**(1): p. 103.
41. Lan, S., et al., *Subgenomic SARS-CoV-2 replicon and reporter replicon cell lines enable ultrahigh throughput antiviral screening and mechanistic studies with antivirals, viral mutations or host factors that affect COVID-19 replication.* bioRxiv, 2021: p. 2021.12.29.474471.
42. He, X., et al., *Generation of SARS-CoV-2 reporter replicon for high-throughput antiviral screening and testing.* Proceedings of the National Academy of Sciences, 2021. **118**(15): p. e2025866118.
43. Addgene. *Plasmid: pLVX-IRES-Puro*.
44. Rawson, J.M.O., et al., *Development of a Cell-Based Luciferase Complementation Assay for Identification of SARS-CoV-2 3CL(pro) Inhibitors.* Viruses, 2021. **13**(2).
45. Thomas, P. and T.G. Smart, *HEK293 cell line: A vehicle for the expression of recombinant proteins.* Journal of Pharmacological and Toxicological Methods, 2005. **51**(3): p. 187-200.
46. Fu, Z., et al., *The complex structure of GRL0617 and SARS-CoV-2 PLpro reveals a hot spot for antiviral drug discovery.* Nature Communications, 2021. **12**(1): p. 488.
47. Aljoundi, A., et al., *Covalent Versus Non-covalent Enzyme Inhibition: Which Route Should We Take? A Justification of the Good and Bad from Molecular Modelling Perspective.* Protein J, 2020. **39**(2): p. 97-105.
48. de Wispelaere, M., et al., *Small molecule degraders of the hepatitis C virus protease reduce susceptibility to resistance mutations.* Nature Communications, 2019. **10**(1): p. 3468.
49. Tedbury, P., in *Personal Communication*.
50. Zhang, H., in *Personal Communication*.